Dynamical Coupling of Rabi Oscillation to Coherent Phonon in Semiconductor Microcavities

K. Mizoguchi, S. Yoshino, and G. Oohata
Department of Physical Science, Osaka Prefecture University, 1-1 Gakuen-cho, Naka-ku, Sakai, Osaka 599-8531, Japan
E-mail address: k.mizoguchi@p.s.osakafu-u.ac.jp

Abstract: We report on the dynamical coupling between Rabi oscillation and coherent phonon in CuCl semiconductor microcavities, which induces the time-dependent frequency-shift of the coherent phonon mode driven by Rabi oscillation.
OCIS codes: (260.7120); (160,6000); (140.3945)

1. Introduction

The study on the dynamical coupling between two oscillations is one of the interesting subjects in ultrafast phenomena [1-4]. When two oscillations at two discrete states coupled to each other are resonant in frequency, it is well known that coupled modes appear, which show an anti-crossing behavior. Quantum beats observed by time-domain spectroscopy originate from quantum interference between two excited states. When the quantum beats are coupled to coherent phonons, the coherent phonons are remarkably enhanced and the coupled modes are observed [3,4]. Since Rabi oscillations observed in semiconductor microcavities also originate from quantum interference between two polariton states, it is expected that the Rabi oscillations will be coupled to coherent phonons through the polarization interaction between the coherent phonon and the excitonic components of polaritons. In this study, we have investigated the coupling dynamics between the Rabi oscillations and coherent phonons in the CuCl semiconductor microcavity.

2. Experiment

The sample used was CuCl semiconductor microcavities with distributed Bragg reflectors (DBRs) consisting of $PbCl_2/AlF_3$ multilayers on Al_2O_3 substrates, as shown in Fig. 1(a) [5]. In a fabricated CuCl microcavity, a cavity layer with the thickness of a cavity length ($L_{cav} = \lambda$) consists of a CuCl active layer with the thickness of $L_{act} = \lambda/8$ sandwiched by AlF_3 spacer layers. Here, λ is given by λ_{ex}/n_b, λ_{ex} is the resonant wavelength of the Z_3 exciton of CuCl in vacuum (λ_{ex} = 387 nm), and n_b is the background refractive index. The transmittance spectra of the CuCl microcavity observed at various incident angles of white light are shown in Fig. 1(b). Three peaks which change with the incident angle show the cavity polariton modes, which are called the lower polariton branch (LPB), the middle polariton branch (MPB) and the upper polariton branch (UPB) in energy order. The peak energies of the cavity polariton modes are plotted as a function of incident angles shown in Fig. 1(c). Three solid curves are the dispersion relationships of the cavity polariton fitted to the experimental results. We focused on the Rabi oscillation between the MPB and LPB, because the energy deference between the MPB and LPB can be controlled over the longitudinal optical (LO) phonon energy of CuCl, E_{LO} = 26 meV (ν_{LO}=6.3 THz) by changing the incident angle of pump pulses in a pump-probe technique. Time-domain signals were measured at 10 K by a transmission-type

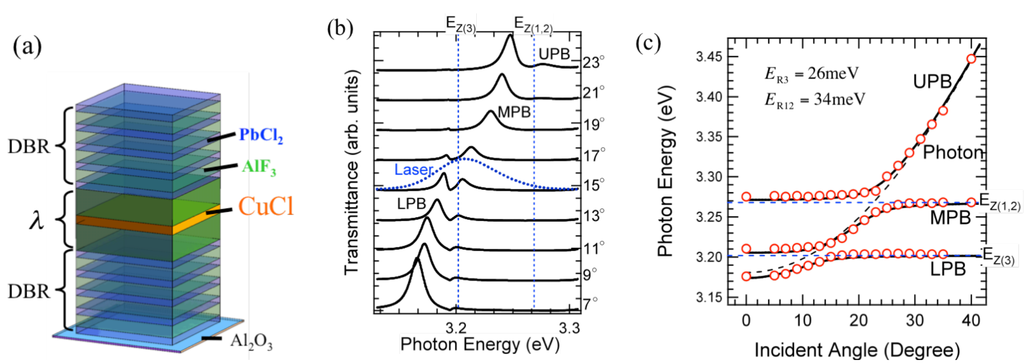

Fig. 1. (a) Schematic of the CuCl microcavity structure. (b) Transmission spectra of the CuCl microcavity for various incident angles at 10 K. The dashed vertical lines denote the energies of the Z_3 and $Z_{1,2}$ excitons: $E_{Z(3)}$ = 3.202 and $E_{Z(1,2)}$ = 3.268 eV, respectively. The dotted blue curve is the laser pulse spectrum. (c) Incident-angle dependence of the peak energies of the cavity polariton modes in the CuCl microcavity (open circles) and dispersion relationship of the cavity polaritons. The estimated Rabi splitting energies for Z_3 and $Z_{1,2}$ excitons are E_{R3}=26 meV and E_{R12}=34 meV, respectively. The dashed curve indicates the dispersion relationship of the cavity photon.

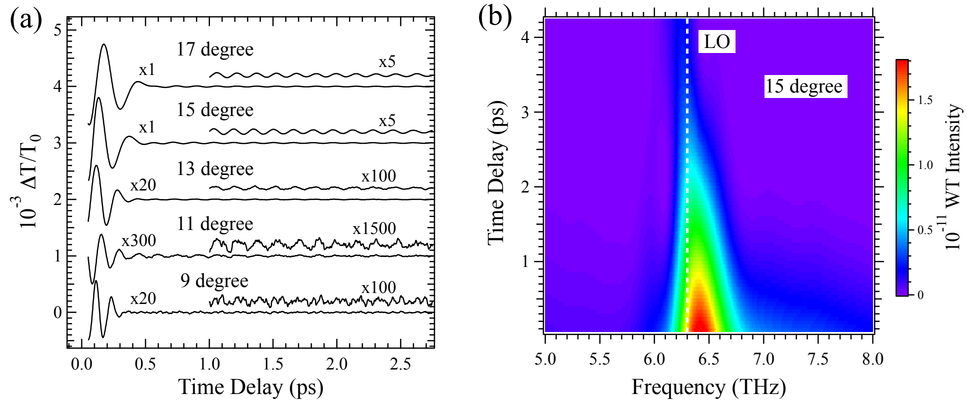

Fig. 2. (a) Time-resolved transmission changes of the CuCl microcavity obtained at various incident angles of pump pulses. (b) Image plots of wavelet transformation (WT) of the coupled oscillation extracted from time domain signals observed at the incident angle of 15 degree. The vertical dotted line indicates the LO phonon frequency of CuCl.

electro-optic (EO) sampling method with second harmonic pulses of a mode-locked Ti:sapphire pulse laser delivering about 90-fs pulse. The center energy of the laser pulses was tuned to 3.207 eV, which was the central energy between the LPB and MPB modes, shown in Fig. 1(b).

3. Experimental Results and Discussion

The time-resolved transmission changes of the CuCl microcavity observed at the various incident angle of pump pulses are shown in Fig. 2(a). The two oscillatory components, which show the strong oscillation with the fast decay time and the weak oscillation with the long decay time, are observed. The short-lived strong oscillation results from the Rabi oscillation between the MPB and LPB, because the period of the strong oscillation changes with the incident angle. On the other hand, the long-lived weak oscillation is related to the coherent LO phonon of CuCl driven by Rabi oscillation, because the frequency of the weak oscillation mode observed in the time-partitioning Fourier transformed spectra after 1 ps is located at about 6.3 THz and the amplitude of the weak oscillation is strengthened with increasing the amplitude of Rabi oscillation.

Now, we consider the coupling between Rabi oscillations and coherent phonons. When we assume that the pump pulse excites only the Rabi oscillation and the coherent phonon is generated by the Rabi oscillation under the weak coupling condition, the oscillation $f(t)$ generated by coupling between two oscillations is given by $f(t)=f_{RO}(t)+f_{C}(t)$, where $f_{RO}(t)$ and $f_{C}(t)$ indicate the Rabi oscillation driven by pump pulses and the coupled oscillation between the Rabi oscillation and coherent phonon, respectively. Then, to reveal the time evolution of the coupled oscillation, we numerically subtracted the Rabi oscillation signals from the observed time-domain signals, and performed the wavelet transformation of the subtracted time-domain signals. The image plots of wavelet transformation (WT) for the pump-pulse incident angle of 15° are shown in Fig. 2(b). It is clear that the frequency of the coupled oscillation mode is shifted to the phonon frequency with increasing the time delay. This result demonstrates that the coupled oscillation mode exists as a coupling state between coherent phonon and Rabi oscillation before Rabi oscillation is relaxed, and the coherent phonon component of the coupled oscillation mode remains after the relaxation of Rabi oscillation.

4. Summary

We have investigated the coupling dynamics between the Rabi oscillation and the coherent LO phonon in the CuCl semiconductor microcavity. The time-domain signals demonstrate that the coupled oscillation generated by coupling between the coherent phonon and Rabi oscillation shows the time-dependent frequency shift.

References

[1] J. Shah, *Ultrafast Spectroscopy of Semiconductors and Semiconductor Nanostructures,* M. Cardona, ed. (Springer, Berlin, 1996).
[2] T. Dekorsy, G. C. Cho and H. Kurz, "Coherent Phonons in Condensed Media" in *Light Scattering in Solids VIII,* M. Cardona and G. Güntherodt, ed. (Springer, Berlin, 2000), Chap. 4.
[3] O. Kojima, K. Mizoguchi and M. Nakayama, "Coupling of coherent longitudinal optical phonons to excitonic quantum beats in GaAs/AlAs multiple quantum wells", Phys. Rev. B **68**, 155325 (2003).
[4] K. Mizoguchi, *et al.*, "Coupled mode of the coherent optical phonon and excitonic quantum beat in GaAs/AlAs multiple quantum wells", Phys. Rev. B **69**, 233302 (2004).
[5] S. Yoshino, *et al.*, "Optical properties of CuCl microcavities with fluctuations in their refractive index profiles along the cavity structures", Phys. Rev. B **88**, 205311 (2013).